MATHEMATICAL BIOSCIENCES
AND ENGINEERING
Volume **8**, Number **1**, January **2011**

doi:10.3934/mbe.2011.8.141

pp. **141–170**

MODELING CONTROL STRATEGIES FOR CONCURRENT EPIDEMICS OF SEASONAL AND PANDEMIC H1N1 INFLUENZA

Olivia Prosper

Department of Mathematics
University of Florida
Gainesville, FL 32611, USA

Omar Saucedo

Department of Mathematics
Texas A&M University
College Station, TX 77843, USA
Current address: Department of Mathematics
University of Florida
Gainesville, FL 32611, USA

Doria Thompson

Department of Mathematics
Spelman College, Atlanta, GA 30314, USA

Griselle Torres-Garcia

School of Human Evolution and Social Change
Mathematical, Computational and Modeling Science Center
Arizona State University, Tempe, AZ 85287, USA

Xiaohong Wang

School of Human Evolution and Social Change
Mathematical, Computational and Modeling Science Center
Arizona State University, Tempe, AZ 85287, USA

Carlos Castillo-Chavez

School of Human Evolution and Social Change
Mathematical, Computational and Modeling Science Center
Arizona State University, Tempe, AZ 85287, USA

2000 *Mathematics Subject Classification.* Primary: 58F15, 58F17; Secondary: 53C35.
Key words and phrases. Seasonal Influenza, Control Theory, Basic Reproductive Number.
This project has been partially supported by grants from the National Science Foundation (NSF - Grant DMPS-0838704), the National Security Agency (NSA - Grant H98230-09-1-0104), the Alfred P. Sloan Foundation and the Office of the Provost of Arizona State University.

Abstract. The lessons learned from the 2009-2010 H1N1 influenza pandemic, as it moves out of the limelight, should not be under-estimated, particularly since the probability of novel influenza epidemics in the near future is not negligible and the potential consequences might be huge. Hence, as the world, particularly the industrialized world, responded to the potentially devastating effects of this novel A-H1N1 strain with substantial resources, reminders of the recurrent loss of life from a well established foe, seasonal influenza, could not be ignored. The uncertainties associated with the reported and expected levels of morbidity and mortality with this novel A-H1N1 live in a backdrop of 36,000 deaths, over 200,000 hospitalizations, and millions of infections (20% of the population) attributed to seasonal influenza in the USA alone, each year. So, as the Northern Hemisphere braced for the possibility of a potentially "lethal" second wave of the novel A-H1N1 without a vaccine ready to mitigate its impact, questions of who should be vaccinated first if a vaccine became available, came to the forefront of the discussion. Uncertainty grew as we learned that the vaccine, once available, would be unevenly distributed around the world. Nations capable of acquiring large vaccine supplies soon became aware that those who could pay would have to compete for a limited vaccine stockpile. The challenges faced by nations dealing jointly with seasonal and novel A-H1N1 co-circulating strains under limited resources, that is, those with no access to novel A-H1N1 vaccine supplies, limited access to the seasonal influenza vaccine, and limited access to antivirals (like Tamiflu) are explored in this study. One- and two-strain models are introduced to mimic the influenza dynamics of a single and co-circulating strains, in the context of a single epidemic outbreak. Optimal control theory is used to identify and evaluate the "best" control policies. The controls account for the cost associated with social distancing and antiviral treatment policies. The optimal policies identified might have, if implemented, a substantial impact on the novel H1N1 and seasonal influenza co-circulating dynamics. Specifically, the implementation of antiviral treatment might reduce the number of influenza cases by up to 60% under a reasonable seasonal vaccination strategy, but only by up to 37% when the seasonal vaccine is not available. Optimal social distancing policies alone can be as effective as the combination of multiple policies, reducing the total number of influenza cases by more than 99% within a single outbreak, an unrealistic but theoretically possible outcome for isolated populations with limited resources.

1. **Introduction.** Influenza is a recurrent infectious disease associated with high morbidity in the human population and, in the case of seasonal influenza, there is a relatively well known pattern of age-specific severity and mortality. Seasonal influenza in the Northern Hemisphere refers to outbreaks that occur approximately between November and April of each year [38]. It is estimated that between 5 and 20 percent of the United States population get the seasonal flu, with approximately 36,000 people dying of flu-related causes each year. Elderly people, young children, and people with specific chronic health conditions have been identified as those *most likely* to develop serious complications from seasonal influenza infections.

Influenza strains that regularly generate outbreaks in human populations are divided into three main types: A, B and C. Type A has a large reservoir since it can infect birds and mammals [33]. Influenza A viruses are differentiated by the structure of their two surface proteins - hemagglutinin (HA) and neuraminidase (NA). Three A-subtypes, H1N1, H2N2, and H3N2, [14] which have afflicted *humans* for centuries, have the ability to maintain an impressive reservoir of genetic variability, primarily through human-to-human transmission and animal reservoirs. Each influenza A subtype gives rise to multiple strains – that is, comparatively minor

variants that result from nucleotide substitutions in the HA molecule. Type A and type B influenza viruses both contribute to the yearly seasonal influenza epidemics in the United States, while type C is less prevalent, causing only mild respiratory illness [16].

Influenza viruses are continuously changing via antigenic shift (major changes) and drift (minor changes) mechanisms [14]. New variants have the ability to evade, or limit the efficacy of, the host's immune system [29]. Mutations often increase the viruses' ability to colonize large populations of individuals. When an individual is infected and recovers from a specific strain of influenza, he/she becomes immune to future infections with the same strain. Furthermore, prior infections with related strains (same subtype) provide different degrees of partial immunity or cross-immunity to new strains within the same subtype [7]. The evolving nature of influenza viruses means vaccines tend to be strongly effective for one year. New vaccines must be prepared each year in order to deal with the emergence of new variants. Vaccine production is therefore based on pre-selected potentially virulent emergent influenza strains. Which strains will be selected in the preparation of the next seasonal vaccine depend on international surveillance and cross-reactivity studies using ferrets [3]. The 2009 seasonal influenza vaccine was a trivalent inactive vaccine (TIV) that included one strain of influenza type B, one of A subtype H1N1 and one of A subtype H3N2 [16]. The pandemic H1N1 vaccine was available (in varying quantities) by December 2009 – that is, most likely too late to be effective [32, 20].

Influenza A has been responsible for several pandemics including the deadly 1918 pandemic and, of course, the 2009-2010 H1N1 (Swine Flu) pandemic [9]. New subtypes (which are rare), are likely to have pandemic potential; new strains (from existing subtypes) capable of escaping detection from most immune systems, also have pandemic potential. The novel H1N1 strain detected in Mexico arose from the recombination of influenza viruses that circulate among pig, avian, and human populations [13]. This kind of reassortment of flu viruses of different species naturally generated high levels of anxiety among public health authorities. Its apparent ability to generate a large number of severe infections among schoolchildren, teenagers, and young adults further increased anxiety in 2009 [12].

The novel H1N1 strain of influenza that surfaced in March 2009 in Mexico has now spread worldwide [12]. Its pattern of mortality was unusual, with 87% of the H1N1-induced deaths having occurred among individuals between the ages of 5 and 59 [12]. The fear that this variant might go through critical genetic changes after visiting the Southern Hemisphere, possibly generating a virulent second wave [36], did not materialize. This novel H1N1 strain infected more people during the winter time (the second wave), that is, during "seasonal influenza" time [5]. Questions and concerns regarding the impact of co-circulating (seasonal and new H1N1) influenza virus surfaced. For example, although the seasonal influenza vaccine included a strain of H1N1, it showed very little, if any, efficacy in reducing infections generated by the novel H1N1 virus [10]. The vaccine for the new H1N1 influenza strain was brought into production rather quickly, distributed unevenly around the world, and most likely arrived too late [21]. The new H1N1 vaccine was made available first to high-risk groups [9], but as the fears associated with H1N1 subsided, countries with large supplies like Canada began to sell large quantities to developing countries like Mexico. The bulk of the vaccine arrived in Mexico in January of 2010. A large percentage of the population, including members of Mexico's medical personnel,

initially refused to get vaccinated [32, 18]. At any rate, distribution took place in large quantities towards the end of January of 2010, probably too late to avoid a catastrophe. Fortunately, the novel A-H1N1 turned out to be relatively "mild".

Although the emergence of the novel H1N1 virus diverted most attention from the seasonal flu, it should be remembered that seasonal influenza poses a significant morbidity and mortality impact every year. In addition, there are resource limitations linked with the effective use and distribution of seasonal influenza vaccines. The United States only had enough seasonal influenza vaccines for roughly one-third of its population [31]. To whom the vaccine should be administered is therefore a relevant public health issue. Research indicates that a large percentage of influenza cases failed to show flu-like symptoms (asymptomatics) [1, 35]. Consequently, a large percentage of individuals receiving the seasonal influenza vaccine might have been (or previously been) asymptomatic with seasonal influenza. Thus, a large proportion of asymptomatics might result in vaccines being wasted. Vaccine-waste is particularly detrimental to countries with limited access to seasonal influenza vaccine stockpiles. These countries must distribute their scarce supplies effectively.

The situation experienced in 2009 regarding the novel A-H1N1 vaccine will repeat itself as seasonal vaccination stockpiles attract the interest of developing nations. The upshot is that rich nations will have greater access than developing nations to antiviral drugs, vaccines, intensive care units, and effective diagnostic tools. Poor nations are likely to have no access to even minimally acceptable medical resources of any type. The development and testing of control policies that make sense in a context that resembles the scenarios faced by poor or developing countries is essential. The research in this manuscript is our attempt to engage the community in this discussion.

Specifically, we explore the use of a seasonal vaccination strategy that asks each patient whether or not he/she has experienced "flu-like" symptoms or received the current seasonal flu vaccine. Individuals that reply "No" are offered the seasonal influenza vaccine. We introduce a model that helps estimate the morbidity and the number of wasted vaccines during an outbreak under the above policy. Optimal control theory is used to identify the policies that minimize morbidity under various scenarios that account for the costs. Specifically, the effectiveness of policies that take into account the cost of social distancing and/or the cost (and availability) of antiviral treatment for the novel H1N1 strain is evaluated. Our paper is organized as follows: In Section 2, we introduce a Susceptible-Asymptomatic-Infected-Recovered (SAIR) model for novel H1N1 influenza and analyzed the effect of H1N1 asymptomatics on disease-dynamics. Optimal control is applied in the context of this SAIR model to determine the "best" way to implement social distancing and treatment, if minimizing cost and the number of H1N1 infections are the priorities. Numerical results and simulations are used to illustrate the characteristics of optimal strategies under selected scenarios. Section 3 introduces a two-strain model that focuses on the competition between seasonal and the novel influenza virus when the seasonal influenza vaccine is available. Further, the optimal control problem is stated in the context of competing strains of influenza and numerical simulations are carried out to identify optimal control policies under various scenarios. Our conclusions and thoughts are summarized in section 4.

2. **SAIR model.**

We first considered a simple SAIR (Susceptible (S) - Asymptomatic (A) - Symptomatic (I) - Recovered (R)) model for novel H1N1 influenza in

which every infected individual first goes through an asymptomatic stage becoming symptomatic at the rate α or recovering without showing symptoms at the rate κ. Since we are less likely to treat asymptomatic individuals, the duration of infection will persist until their immune system takes over.

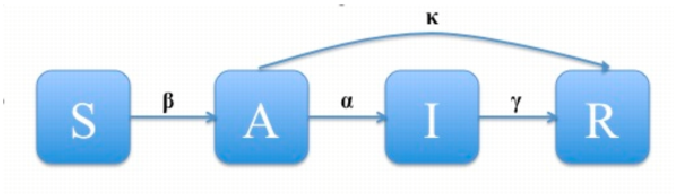

FIGURE 1. Diagram of the SAIR compartmental model.

Some definitions are introduced to describe the SAIR model. The state variable S denotes the susceptible individuals; A denotes the asymptomatic-infectious; I the symptomatic-infectious; and R denotes the recovered – that is, those individuals that gain full immunity after infection. The model parameters β, α, γ, and κ quantify the rate of an individual's progression from one state to the next. Specifically, β denotes the per-susceptible per-infected transmission rate; α is the per-capita progression rate from the asymptomatic to the symptomatic class; γ is the per-capita recovery rate of the symptomatic class; and κ is the per-capita recovery rate of asymptomatics. Births and deaths are ignored in this section. Consequently, the size of the population $N = S + A + I + R$ is constant. Susceptible individuals may become infected by coming into contact with either an asymptomatic or symptomatic individual. Although asymptomatic individuals are likely less infectious than symptomatic individuals, we assume for simplicity that asymptomatics and symptomatics are equally infectious. These assumptions and definitions lead to the following single outbreak epidemic $SAIR$ model:

$$\begin{aligned}
\frac{dS}{dt} &= -\beta S\frac{A+I}{N} && (1)\\
\frac{dA}{dt} &= \beta S\frac{A+I}{N} - (\alpha+\kappa)A && (2)\\
\frac{dI}{dt} &= \alpha A - \gamma I && (3)\\
\frac{dR}{dt} &= \gamma I + \kappa A && (4)\\
N &= S + A + I + R, && (5)
\end{aligned}$$

where individuals are assumed to mix uniformly.

The basic reproductive number [2], that is, the average number of secondary infections generated by the introduction of a typical infectious individual (a mixture of asymptomatics and symptomatics) in a population where $S \approx N$ is given by

$$R_0 = R_A + R_I,$$

where $R_A = \frac{\beta}{\alpha+\kappa}$ denotes the contribution to secondary infections by the A-class and $R_I = \frac{\beta}{\alpha+\kappa}\frac{\alpha}{\gamma}$ the relevant contribution by the I-class.

Using the approaches found in Brauer et al [6], we arrive at the following final size relationship for the single-strain and single outbreak model:

$$\ln\left(\frac{S_0}{S_\infty}\right) - R_0\left(1 - \frac{S_\infty}{N}\right) = 0, \tag{6}$$

where S_0 denotes $S(0)$ and S_∞ denotes the size of the susceptible population at the end of the outbreak. Relation (6) determines the connection between R_0 and the total number of individuals who became infected ($N - S_\infty$). This implicit relationship (6) allows, for example, for the use of serological studies to estimate R_0 through the use of estimates of the actual infected proportion in the population, after a single outbreak is over.

2.1. **SAIR model with control.** Control theory is used to identify ways of producing maximum performance at a minimal cost under various sets of assumptions [34]. Control theory has been used to evaluate the effectiveness (including the cost) of "case finding" – the identification of an infected individual together with cost-effective interventions that produce a faster (individual and population) recovery [22]. Case finding, in the context of our SAIR model, would correspond to the treatment of individuals identified as infected, with antiviral drugs. Control theory is also used to reduce the length and number of infections. The activities and techniques used to avoid contracting an infection are often referred to as "case holding" [22]. We address case holding measures in our setting through the addition of potentially costly social distancing measures like closing schools or public events. Lee et al. [24] address the use of antivirals drugs and social distancing in their single-strain pandemic model via controls that reduce the number of contacts between susceptible and hospitalized individuals [24]. Mexico implemented case-finding and case-holding measures during the months of April and May, 2009 in their efforts to reduce the impact of the novel H1N1 virus [17]. The economic cost derived from the implementation of Mexico's policies was tremendous [24].

Deploying all methods of disease control at full force is likely to be effective in stopping an influenza outbreak but far too costly. Further, the effective implementation of social distancing measures over larger windows in times is most likely impossible. So, what are the best means for controlling the size of an outbreak such as the one generated by novel H1N1 in Mexico? What is the best way to implement control measures? Through the incorporation of two time-dependent controls to Model 1 we address these questions theoretically. The control $u_1(t)$ measures the effort needed to increase social distancing, reducing the effective transmission rate (β). The control $u_2(t)$ measures the effort required in administering antiviral drug treatment to novel H1N1 infected individuals. Both control functions are required to be bounded and Lebesgue integrable on the interval $[0, t_f]$, where t_f denotes a pre-selected length of time during which these controls are applied. We only treat symptomatic individuals. Hence, the term $\gamma_T u_2(t)$, where γ_T is the additional recovery rate of a novel H1N1 infected individual undergoing treatment (i.e. $\gamma + \gamma_T$ = recovery rate with treatment), is inserted. Wherever a full effort is being placed on social distancing or treatment measures at time t, we would have that $u_1(t)$ and $u_2(t)$ must be equal to one. Likewise, the situation when $u_1(t)$ and $u_2(t)$ are equal to zero corresponds to the situation when no effort is being placed in these controls at time t.

The above observations leads to the following model with two controls:

$$\begin{aligned}
\frac{dS}{dt} &= -\beta(1-u_1(t))S\left(\frac{A+I}{N}\right) \\
\frac{dA}{dt} &= \beta(1-u_1(t))S\left(\frac{A+I}{N}\right) - (\alpha+\kappa)A \\
\frac{dI}{dt} &= \alpha A - (\gamma+\gamma_T u_2(t))I \\
\frac{dR}{dt} &= (\gamma+\gamma_T u_2(t))I + \kappa A.
\end{aligned} \tag{7}$$

Naturally, each control incurs in some costs: social distancing generates economic losses and effective treatment requires the existence and support of a costly public health infrastructure. Unfortunately, we do not have good data on the costs associated with these efforts (although there are some studies which attempt to quantify the cost of antiviral treatment [23]). Hence, we focus on the use of "relative" cost for the controls. We use the quadratic term $\frac{B_1}{2}u_1^2 + \frac{B_2}{2}u_2^2$, where the constant B_i represents the weight constant for the control u_i (i=1,2) and $\frac{B_1}{B_2}$ is the relative cost of u_1 with respect to u_2. We make the a priori assumption that social distancing is more costly than treatment, which may be true in some societies. Minimizing the total number of infections during the H1N1 outbreak is the pre-selected goal. The minimization of an objective functional J, that incorporates both infectious classes (A and I) and their costs is the selected approach. J, a function of the controls, is defined by

$$J(u_1(t), u_2(t)) = \int_0^{t_f} \left(A + I + \frac{B_1}{2}u_1^2 + \frac{B_2}{2}u_2^2\right) dt. \tag{8}$$

The problem becomes that of finding a pair of functions (u_1^*, u_2^*) such that

$$J(u_1^*, u_2^*) = min_\Omega J(u_1, u_2), \tag{9}$$

where, for $i = 1, 2$ and LB_i and UB_i fixed constants in $[0, 1]$,

$$\Omega \equiv \{(u_1(t), u_2(t)) \in L^1(0, t_f) \| LB_i \leq u_i(t) \leq UB_i, t \in [0, t_f]\}, \tag{10}$$

subject to the State Equations (7) for a given set of initial conditions. The pair of function (u_1^*, u_2^*) are the optimal controls.

The existence of optimal controls u_1^* and u_2^* for this model is guaranteed by standard results in Optimal Control Theory [19]. Necessary conditions that the controls must satisfy are derived via Pontryagin's Maximum Principle. The optimal control problem given by expressions (7)-(10) is equivalent to that of minimizing the Hamiltonian H:

$$\begin{aligned} H &= A + I + \frac{B_1}{2}u_1^2 + \frac{B_2}{2}u_2^2 \\ &+ \lambda_1\left(-\beta(1-u_1(t))S\left(\frac{A+I}{N}\right)\right) \\ &+ \lambda_2\left(\beta(1-u_1(t))S\left(\frac{A+I}{N}\right) - (\alpha+\kappa)A\right) \\ &+ \lambda_3\left(\alpha A - (\gamma+\gamma_T u_2(t))I\right) \\ &+ \lambda_4\left((\gamma+\gamma_T u_2(t))I + \kappa A\right) \end{aligned}$$

A standard application of Pontryagin's Maximum Principle [30] leads to the following result:

Theorem 2.1. *There exists an optimal pair $u_1^*(t), u_2^*(t)$ and corresponding solutions, S^*, A^*, I^*, and R^*, that minimizes $J(u_1(t), u_2(t))$ over Ω. The explicit optimal controls are connected to the existence of continuous specific functions $\lambda_i(t)$, the solutions of the following adjoint system:*

$$\begin{aligned} \frac{d\lambda_1}{dt} &= \lambda_1\beta(1-u_1(t))\left(\frac{A+I}{N}\right) - \lambda_2\beta(1-u_1(t))\left(\frac{A+I}{N}\right) \\ \frac{d\lambda_2}{dt} &= -1 + \lambda_1\beta(1-u_1(t))\frac{S}{N} - \lambda_2\left(\beta(1-u_1(t))\frac{S}{N} - (\alpha+\kappa)\right) \\ &\quad -\lambda_3\alpha - \lambda_4\kappa \\ \frac{d\lambda_3}{dt} &= -1 + \lambda_1\beta(1-u_1(t))\frac{S}{N} - \lambda_2\beta(1-u_1(t))\frac{S}{N} + \lambda_3(\gamma+\gamma_T u_2(t)) \\ &\quad -\lambda_4(\gamma+\gamma_T u_2(t)) \\ \frac{d\lambda_4}{dt} &= 0 \end{aligned} \tag{11}$$

subject to the transversality conditions,

$$\lambda_i(t_f) = 0 \text{ for all } i = 1, 2, 3, 4. \tag{12}$$

Furthermore, the following properties hold

$$\begin{aligned} u_1^* &= min\left(max\left(LB_1, \frac{1}{B_1}\left[\beta S\left(\frac{A+I}{N}\right)(\lambda_2-\lambda_1)\right]\right), UB_1\right) \\ u_2^* &= min\left(max\left(LB_2, \frac{1}{B_2}\left[\gamma_T I(\lambda_3-\lambda_4)\right]\right), UB_2\right), \end{aligned} \tag{13}$$

2.1.1. *Numerical Results.* Numerical simulations leading to the approximation of the optimal controls, are carried out using the forward Euler method. Starting with an initial guess for the value of the controls on the time interval $[0, t_f]$, we solve the state system with controls (7) using forward Euler. Next, the adjoint system is solved using the solutions of the state system and the transversality conditions (12) backward in time. After updating the controls u_1 and u_2, the error between the old values of u_i $(i = 1, 2)$ and the updated values is calculated. The process is repeated until the error is less than a pre-assigned value (here chosen to be 0.001). The final values of u_1 and u_2 obtained via the above method are the numerical approximations to the optimal control pair (u_1^*, u_2^*). There are several

means of updating the values of the controls u_1 and u_2 after each iteration. In our case, to avoid convergence problems, it was necessary to use a convex combination with a weighted average (regardless of the values chosen for B_1 and B_2) [25]. Representative simulations using the parameter values for H1N1 specified in Table 2, including the basic reproductive number $R_0 = 1.8$, are used to highlight the results of applying optimal controls in three scenarios. In the first scenario, the optimal strategy when social distancing and treatment control measures are implemented simultaneously is illustrated. The second scenario considers social distancing without treatment. In scenarios one and two we arbitrarily fix the cost constant for treatment, B_2, to the value 10. We simulate the optimal solutions when $B_1 = 20$, 30, and 50. Finally, the third scenario highlights the results of computing the optimal strategy when treatment is the only control with values of $B_2 = 10$, 100, 1000, and 10,000.

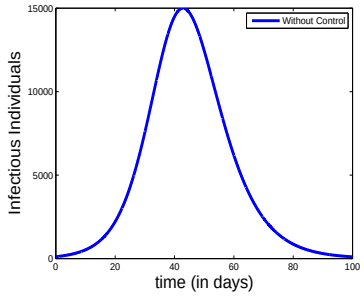

(a) Number of infections $(A + I)$ at time t without control

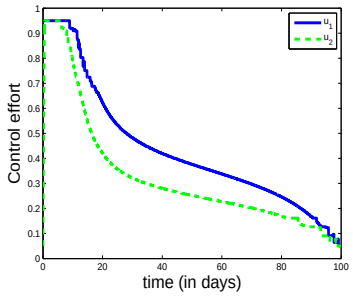

(b) Optimal control functions u_1 and u_2

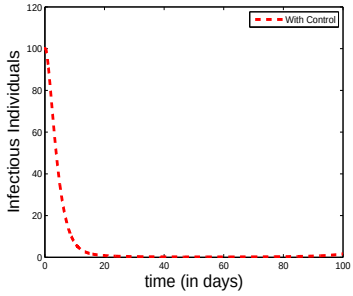

(c) Number of infections $(A + I)$ at time t with control

FIGURE 2. SAIR optimal control results for the case where $\frac{B_1}{B_2} = 2$ and $A(0) = 100$. Figure (a) illustrates the SAIR model outbreak $(A + I)$ without control. The optimal control functions are plotted in (b), and (c) demonstrates the impact of the optimal control policy on the influenza outbreak $(A + I)$.

The dynamics of the natural single outbreak are plotted in Figure 2(a). That is, Figure 2(a) illustrates the course of the epidemic in the absence of controls, with parameter values $\beta = \beta_2$, $\alpha = \alpha_2$, $\gamma = \gamma_2$ from Table 2, and $\kappa = \mu = 0$. The parameter values chosen are consistent with the parameter values used for the novel H1N1 virus in the two-strain model introduced in the next section.

First, we seek the optimal strategy when social distancing and treatment control measures are implemented concurrently. The numerical solutions, $u_1(t)$ and $u_2(t)$ where social distancing is twice as costly as treatment ($B_1 = 20$ and $B_1 = 10$) are presented in Figure 2(b). The computed optimal control strategy requires maximum effort at the beginning of the outbreak. This result is consistent with the observations of Horst Behncke in his study of optimal control applied to deterministic SIR epidemic models [4].

We observe from Figures 2(b) and 2(c), where $B_1 = 20$ and $B_1 = 10$, that the implementation of the optimal controls (social distancing and treatment) immediately suppresses the outbreak. The use of optimal controls requires strong efforts at the beginning of the outbreak. It is not surprising that they are quite effective at yielding immediate positive results. Social distancing is the most costly control (by assumption) and yet, Figure 2(b) says that most of the effort should be placed in social distancing, not on treatment, throughout the outbreak. Mexican authorities used social distancing measures, closing schools, restaurants, and public events, to mitigate the potential of the novel H1N1 pandemic [17] – a very expensive proposition that led to hotel occupancy levels of 10% in Mexico City [26]. Comparisons between the sizes of the spring and fall wave [21] suggest that they worked.

Increasing the relative cost of the control u_1 by setting $B_1 = 50$ while keeping B_2 fixed so that $\frac{B_1}{B_2} = 5$, (social distancing five times more costly than treatment) leads to an optimal control policy that puts more effort into treatment. Thus, the higher the relative cost of u_1, the less the benefits associated with the use of this control when cost is factored in. In general, as $\frac{B_1}{B_2}$ increases, the number of novel A-H1N1 cases increases. However, for $\frac{B_1}{B_2} = 2$, 3, and 5, using the optimal control policy reduced the number of cases by more than 99%.

How effective would a single control policy be? That is, what would be the optimal effort required if we were only to implement one control strategy at a time? A significant reduction in the size of the outbreak is still observed when social-distancing is the sole control measure and $B_1 = 20$. The implementation of the optimal control requires intense effort for the first 20 days, which might be difficult to achieve in practice. Most often, policies are implemented sometime after the start of an outbreak since the immediate implementation is often impossible. Delays are the "worst" enemies if the goal is to reduce the morbidity of "fast" drivers like influenza [24]. In the case of Mexico, school closures began on April 23rd, 2009, 6 days after the outbreak was identified [17] while in Japan, control policies came into effect on May 18th, 9 days after the start of the outbreak [27]. In other words, national responses were fast and yet often too late [27].

Finally, Figure 3(a) highlights the exclusive use of treatment as a control measure with weight constant $B_2 = 10$. This last policy is not as effective as social distancing alone. We see that treatment alone reduces the total morbidity by 63% with more than 99% reduction when the optimal social distancing strategy is employed. In fact, the outbreak continues when treatment is the sole optimal control measure over a 100-day horizon. In the case where $\frac{B_1}{B_2} = 100$, the optimal control function and the resulting influenza outbreak are qualitatively very similar to the case where $\frac{B_1}{B_2} = 100$. However, as the cost of treatment increases further, we observed dramatic differences in the shape of the optimal treatment control function u_2 (Figure 3), including a decline in efficacy. In fact, the efficacy (in terms of the percent reduction in the number of cases during the control period) of this single control strategy is roughly 62% if B_2 equals 100 or 1000 and decreases dramatically to 30% if treatment

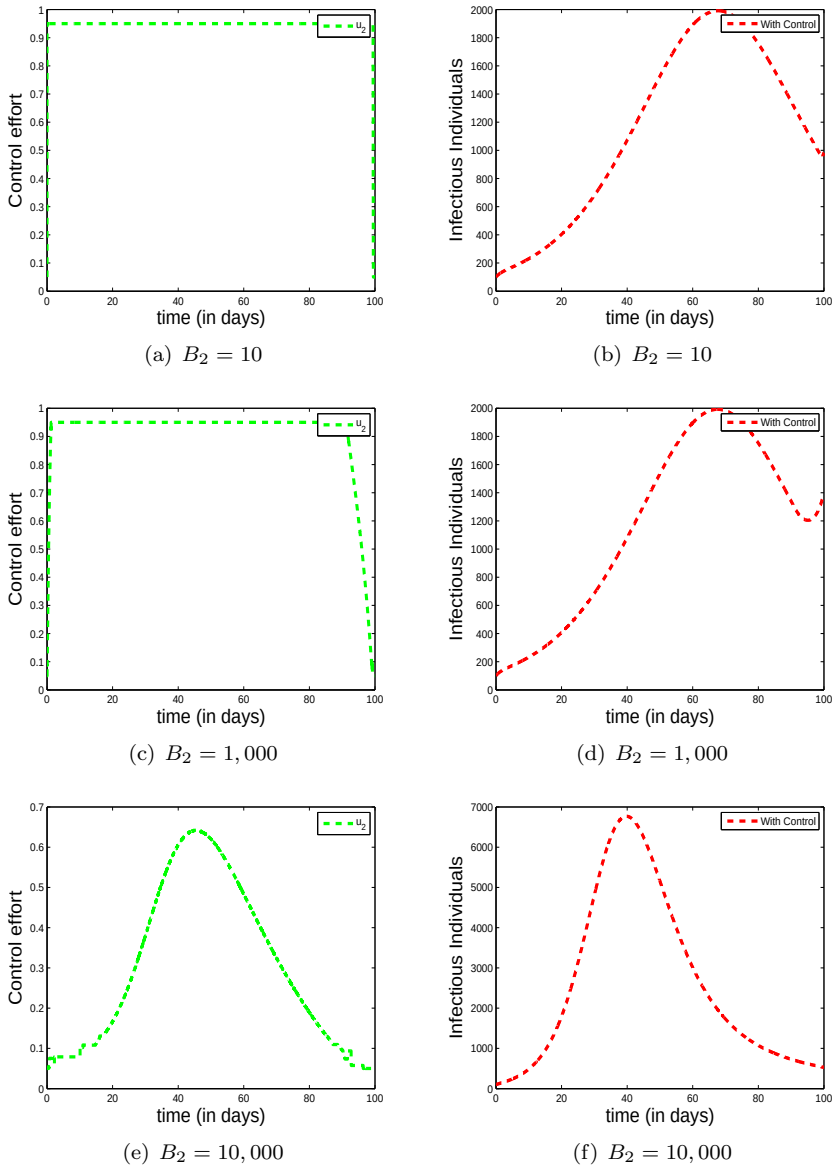

(a) $B_2 = 10$ (b) $B_2 = 10$

(c) $B_2 = 1,000$ (d) $B_2 = 1,000$

(e) $B_2 = 10,000$ (f) $B_2 = 10,000$

FIGURE 3. SAIR optimal control results for treatment-only strategy with $A(0) = 100$ and $B_2 = 10$, 1,000, and 10,000. (a), (c), and (e) illustrate the optimal treatment-only control functions. (b), (d), and (f) demonstrate the number of infections ($A+I$) over time resulting from the corresponding optimal control policy.

is very costly ($B_2 = 10000$). Behnke observed that in his applications of optimal control theory to SIR models, the optimal control solution always appeared to be one in which maximum effort was required at the beginning of the outbreak [4]. However, the shape of u_2 if $B_2 = 10000$ (Figure 3(e)), in the absence of social distancing, differs substantially from Behnke's observation. Instead, the optimal

treatment-only policy follows the similar "hill-like "shape of the outbreak. The corresponding curves illustrating the number of infections at time t $(A(t)+I(t))$ for each case are presented in Figures 3(b), 3(d), and 3(f).

3. **Co-circulating influenza strains.** As expected, the incidence of cases of novel H1N1 accelerated as it moved to the Southern Hemisphere. The emergence of the novel strain of H1N1 in April of 2009 in the Northern Hemisphere and the large scale social distancing measures put in place, for example in China, Japan, and North America, meant that, despite the (suspected) large number of individuals with asymptomatic infections, the population of individuals susceptible to H1N1 probably remained high. Epidemic data from several countries in the Northern Hemisphere (including North America) have confirmed that a large pool of susceptibles remained. In Mexico, for example [21], three waves were observed in the number of reported cases of the novel H1N1: the initial spring wave, a smaller summer wave, and a huge fall wave. The third waves in Canada, Mexico, and the US, emerged as the seasonal H1N1 vaccine was being delivered. Data show [21] that most of the reported cases of influenza in the fall and winter of 2009 can be directly attributed to the novel H1N1, which appears to have "out-competed" the seasonal flu. It is therefore not far fetched to assume that the availability and wide distribution (at least in Canada and the US) of the seasonal influenza vaccine may have indeed helped the novel H1N1 "out-compete" the seasonal flu.

In this section, an influenza dynamics framework that allows the exploration of the time evolution of the (joint) dynamics of the novel H1N1 and seasonal influenza, mediated by the distribution of the seasonal influenza vaccine and the availability of antiviral drugs, is introduced.

It is assumed that everyone is susceptible to both strains of influenza before a joint outbreak is experienced. Further, co-infections are ignored since the average infectious period is short. Individuals that recover from their first influenza infection become immediately susceptible to infection by the alternate type. It is assumed that only the seasonal influenza vaccine is available and that there is no cross-immunity between the novel H1N1 and the seasonal "flu". Infected individuals die or recover with permanent immunity to infection to the same "flu"; we do not assume that the population size is constant. Natural births and deaths are not considered, since our interest is on the joint dynamics over a short window in time. The seasonal vaccine is assumed to be 100% effective while the influenza recovery rates are assumed to be different. Asymptomatics (A) as well as symptomatics (I) are considered in the model because, by all accounts, they seem to play a vital role in disease transmission [1, 35].

In order to simplify the analysis here, it is assumed that all infected individuals experience an asymptomatic period followed by an infectious period (Figure 4). Individuals who do not show symptoms will be given the seasonal vaccine. This assumption leads to three vaccinated classes: vaccinated susceptibles (V_S), vaccinated individuals with asymptomatic seasonal influenza infection (V_{A1}), and vaccinated individuals with asymptomatic novel H1N1 influenza infection (V_{A2}). Vaccinated individuals are not considered immune to the novel H1N1 virus. This assumption leads to several infected (and infectious) classes: asymptomatic novel H1N1 infections that had a prior seasonal influenza infection $(A_{1,2})$, symptomatic novel H1N1 infections that had a prior seasonal influenza infection $(I_{1,2})$, asymptomatic

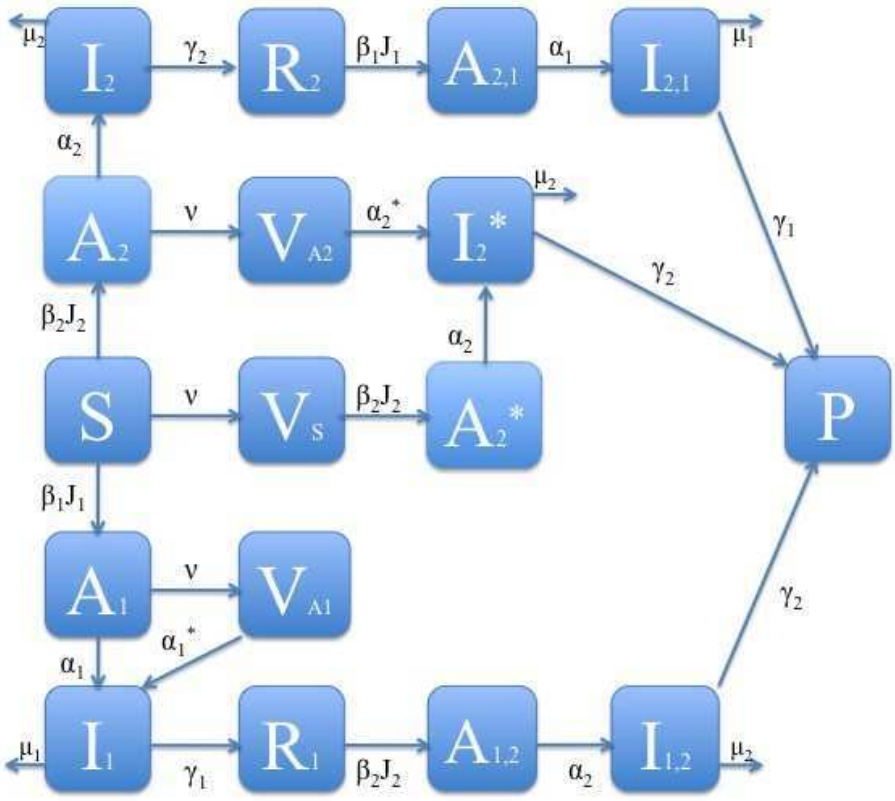

FIGURE 4. Diagram of the compartmental model, where 1 =Seasonal and 2 =H1N1.

seasonal influenza infections that had a prior novel H1N1 infection ($A_{2,1}$), symptomatic seasonal influenza infections that had a prior novel H1N1 infection ($I_{2,1}$), asymptomatic H1N1 infected individuals who were vaccinated but have no prior infections (A_2^*), and novel H1N1 infections (I_2^*) that develop symptoms after passing through either V_{A2} or A_2^*. Individuals in the symptomatic classes die or move on to the protected class (P) – protected against re-infection from both strains. The class V_{A1} keeps track of asymptomatic seasonal influenza infected individuals who received the seasonal flu vaccine. Since seasonal asymptomatic individuals are still infectious and will eventually show symptoms, any seasonal influenza vaccine given to them is wasted.

Controls are used to manage social distancing (u_1) and antiviral treatment (u_2) as it was done in the single-strain influenza model. Vaccination is not managed via controls; it is assumed that the vaccination policy described above is in place and that the cost associated with such a policy is known. Further, we keep track of "wasted" vaccines under the "asymptomatics-only" seasonal influenza vaccination policy. These assumptions lead to the following model:

TABLE 1. List of epidemiological classes and their meaning, where 1 = Seasonal and 2 = H1N1

Class	Meaning
S	Susceptible
A_1	Infected with Seasonal- Not Showing Symptoms (No Previous Infection)
I_1	Infected with Seasonal - Showing Symptoms (No Previous Infection)
R_1	Recovered from Seasonal
A_2	Infected with H1N1- Not Showing Symptoms (No Previous Infection)
I_2	Infected with H1N1 - Showing Symptoms (No Previous Infection)
R_2	Recovered from H1N1
V_s	Vaccine Given to Susceptible
V_{A1}	Vaccine Given to Asymptomatic with Seasonal Flu
V_{A2}	Vaccine Given to Asymptomatic with H1N1 Virus
A_2^*	Infected with H1N1 after Receiving Vaccine- Not Showing Symptoms
I_2^*	Infected with H1N1 after Receiving Vaccine- Showing Symptoms
$A_{1,2}$	Previously Infected with Seasonal, now Infected with H1N1 - Not Showing Symptoms
$A_{2,1}$	Previously Infected with H1N1, now Infected with Seasonal - Not Showing Symptoms
$I_{1,2}$	Previously Infected with Seasonal, now Infected with H1N1 - Showing Symptoms
$I_{2,1}$	Previously Infected with H1N1, now Infected with Seasonal - Showing Symptoms
P	Protected Against Seasonal and H1N1

$$\frac{dS}{dt} = -\beta_1(1-u_1)SJ_1 - \beta_2(1-u_1)SJ_2 - \nu S \tag{14}$$

$$\frac{dA_1}{dt} = \beta_1(1-u_1)SJ_1 - (\alpha_1+\nu)A_1 \tag{15}$$

$$\frac{dI_1}{dt} = \alpha_1 A_1 + \alpha_1^* V_{A1} - (\gamma_1+\mu_1)I_1 \tag{16}$$

$$\frac{dR_1}{dt} = \gamma_1 I_1 - \beta_2(1-u_1)R_1 J_2 \tag{17}$$

$$\frac{dA_{1,2}}{dt} = \beta_2(1-u_1)R_1 J_2 - \alpha_2 A_{1,2} \tag{18}$$

$$\frac{dI_{1,2}}{dt} = \alpha_2 A_{1,2} - (\gamma_2(1+u_2)+\mu_2)I_{1,2} \tag{19}$$

$$\frac{dA_2}{dt} = \beta_2(1-u_1)SJ_2 - (\alpha_2+\nu)A_2 \tag{20}$$

$$\frac{dI_2}{dt} = \alpha_2 A_2 - (\gamma_2(1+u_2)+\mu_2)I_2 \tag{21}$$

$$\frac{dR_2}{dt} = \gamma_2(1+u_2)I_2 - \beta_1(1-u_1)R_2 J_1 \tag{22}$$

$$\frac{dA_{2,1}}{dt} = \beta_1(1-u_1)R_2 J_1 - \alpha_1 A_{2,1} \tag{23}$$

$$\frac{dI_{2,1}}{dt} = \alpha_1 A_{2,1} - (\gamma_1+\mu_1)I_{2,1} \tag{24}$$

$$\frac{dV_{A2}}{dt} = \nu A_2 - \alpha_2^* V_{A2} \quad (25)$$
$$\frac{dI_2^*}{dt} = \alpha_2^* V_{A2} + \alpha_2 A_2^* - (\gamma_2(1+u_2)+\mu_2)I_2^* \quad (26)$$
$$\frac{dV_S}{dt} = \nu S - \beta_2(1-u_1)V_S J_2 \quad (27)$$
$$\frac{dA_2^*}{dt} = \beta_2(1-u_1)V_S J_2 - \alpha_2 A_2^* \quad (28)$$
$$\frac{dV_{A1}}{dt} = \nu A_1 - \alpha_1^* V_{A1} \quad (29)$$
$$\frac{dP}{dt} = \gamma_2(1+u_2)(I_2^* + I_{1,2}) + \gamma_1 I_{2,1} \quad (30)$$

where

$$J_1 = \frac{I_1 + A_1 + A_{2,1} + I_{2,1} + V_{A_1}}{N}$$
$$J_2 = \frac{I_2 + A_2 + A_{1,2} + I_{1,2} + I_2^* + A_2^* + V_{A2}}{N}$$

The dynamics of the above model are first explored without controls. The basic reproductive number under vaccination, R_v ([37, 15]) is given by

$$R_v = max\{R_{01v}, R_{02v}\},$$

where

$$R_{01v} = \frac{\beta_1}{\alpha_1+\nu} + \frac{\beta_1}{\alpha_1+\nu}\frac{\alpha_1}{\gamma_1+\mu_1} + \frac{\beta_1}{\alpha_1+\nu}\frac{\nu}{\alpha_1^*}\frac{\alpha_1^*}{\gamma_1+\mu_1} + \frac{\beta_1}{\alpha_1+\nu}\frac{\nu}{\alpha_1^*}$$
$$R_{02} = \frac{\beta_2}{\alpha_2+\nu} + \frac{\beta_2}{\alpha_2+\nu}\frac{\alpha_2}{\gamma_2+\mu_2} + \frac{\beta_2}{\alpha_2+\nu}\frac{\nu}{\alpha_2^*}\frac{\alpha_2^*}{\gamma_2+\mu_2} + \frac{\beta_2}{\alpha_2+\nu}\frac{\nu}{\alpha_2^*}.$$

In the absence of vaccination, R_v reduces to the basic reproductive number, R_0. Thus, the basic reproductive numbers for seasonal influenza and H1N1 are

$$R_{01} = \frac{\beta_1}{\alpha_1} + \frac{\beta_1}{\alpha_1}\frac{\alpha_1}{\gamma_1+\mu_1}$$
$$R_{02} = \frac{\beta_2}{\alpha_2} + \frac{\beta_2}{\alpha_2}\frac{\alpha_2}{\gamma_2+\mu_2},$$

respectively. Thus, $R_0 = max\{R_{01}, R_{02}\}$.

The terms in R_{01v} and R_{02v} represent secondary infections generated by infectious individuals with different "life" histories. R_{01v} denotes the average number of secondary infections generated by a "typical" seasonal influenza infected individual in a population that includes vaccinated individuals in the absence of treatment and social-distancing measures. Specifically, $\frac{\beta_1}{\alpha_1+\nu}$ denotes the secondary infections generated by the A_1 class; $\frac{\beta_1}{\alpha_1+\nu}\frac{\alpha_1}{\gamma_1+\mu_1}$ denotes the secondary infections coming from non-vaccinated individuals in the I_1 class; $\frac{\beta_1}{\alpha_1+\nu}\frac{\nu}{\alpha_1^*}\frac{\alpha_1^*}{\gamma_1+\mu_1}$ denotes the secondary infections arising from vaccinated individuals in the I_1 class; and $\frac{\beta_1}{\alpha_1+\nu}\frac{\nu}{\alpha_1^*}$ denotes the secondary infections generated by individuals in the V_{A1} class. Similarly, R_{02} denotes the average number of secondary infections generated by a "typical "novel H1N1 influenza infected individual in a population that includes vaccinated individuals in the absence of treatment and social-distancing measures. In the term R_{02v},

$\frac{\beta_2}{\alpha_2+\nu}$ denotes the secondary infections generated by individuals in A_2; $\frac{\beta_2}{\alpha_2+\nu}\frac{\alpha_2}{\gamma_2+\mu_2}$ denotes the secondary infections generated by individuals in I_2; $\frac{\beta_2}{\alpha_2+\nu}\frac{\nu}{\alpha_2^*}\frac{\alpha_2^*}{\gamma_2+\mu_2}$ denotes the secondary infections generated by individuals in I_2^*; and $\frac{\beta_2}{\alpha_2+\nu}\frac{\nu}{\alpha_2^*}$ denotes the secondary infections generated by individuals in A_2^*.

TABLE 2. List of epidemiological parameters and their values. These parameter values represent the values used in all of the numerical simulations presented in this paper. Transmission rates are calculated using the formulation of R_{01} and R_{02} and the remaining parameter values given in this table. For simplicity we assume the disease-induced death rates μ_1 and μ_2 are zero, although in reality they are non-zero. Parameter values (other than for R_{01} and R_{02}) without citations are rough estimates based on general CDC information regarding influenza. The units for all parameters other than R_{01} and R_{02} are $days^{-1}$ Index 1 refers to Seasonal Influenza and index 2 to the Novel H1N1 influenza.

Parameters	Description	Value	Reference
β_1	Transmission Rate	0.2167	Estimate
α_1	Rate of Progression to Symptomatic	$\frac{1}{2}$	Estimate
α_1^*	Rate to Symptomatic Infection after Vaccination	.5	Estimate
γ_1	Recovery Rate	$\frac{1}{5}$	[8]
μ_1	Death Rate	0	
ν	Vaccination Rate	.01	Estimate
R_{01}	Basic Reproductive Number	1.3	[11]
β_2	Transmission Rate	0.2793	Estimate
α_2	Rate of Progression to Symptomatic	$\frac{1}{2}$	[28]
α_2^*	Rate to Symptomatic Infection after Vaccination	.5	Estimate
γ_2	Recovery Rate	$\frac{1}{33}$: $\frac{1}{100}$	[28]
μ_2	Death Rate	0	
R_{02}	Basic Reproductive Number	1.8	[28]

From the definition of R_v, we arrive at four cases: $R_{01v} > 1$ and $R_{02v} > 1$ (simultaneous seasonal and novel H1N1 outbreaks occur), $R_{01v} < 1$ and $R_{02v} > 1$ (only novel H1N1 outbreak occurs), $R_{01v} > 1$ and $R_{02v} < 1$ (only seasonal influenza outbreak occurs), and $R_{01v} < 1$ and $R_{02v} < 1$ (neither seasonal nor novel H1N1 result in an outbreak). Using the parameter values given in Table 2, our two-strain influenza model falls under the first case, that is, in which an outbreak of both seasonal and novel H1N1 occur simultaneously. This is the only scenario explored.

3.1. **Simulations of a concurrent influenza outbreak with and without vaccination, in the absence of social distancing and treatment measures.** Numerical simulations, generated using the parameter values listed in Table 2, are used to evaluate the effects of vaccination on the duration of an outbreak, the total morbidity at the end of the seasonal and novel H1N1 influenza outbreaks, and the total number of wasted vaccines during an outbreak. In particular, since the basic

reproductive number is given by $R_0 = max\{R_{01}, R_{02}\}$, $R_0 = 1.8$. We present results for a population size of 100,000 and different initial conditions.

Figure 5 plots the outbreaks of seasonal and novel H1N1 influenza for different initial conditions in the absence of a vaccination policy. The graphs demonstrate a much larger peak in the novel H1N1 outbreak than for seasonal influenza; however, the duration of the novel H1N1 outbreak is much shorter. We observed different dynamics in the growth of the A_1 class in Figures 5(a) and 5(c). When there are more asymptomatic seasonal infections than asymptomatic novel H1N1 infections at the beginning of the outbreak, we noticed fluctuations in the growth of A_1. Initially, A_1 increases then begins to decrease as individuals recover from seasonal influenza. Then, as individuals recover from I_2, they are now susceptible to a secondary infection from a seasonal virus. Because the novel H1N1 outbreak is large, the number of secondary seasonal infections is greater than the number of primary seasonal infections. So, as members of the population enter the A_{21} class, they begin to infect members of class S, resulting in another visible increase in the A_1 class.

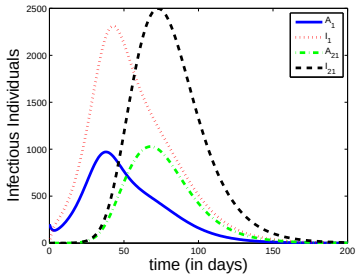

(a) Seasonal Infectious classes. $R_{01} > 1$.

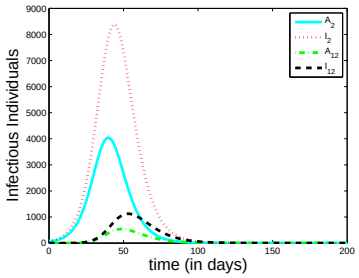

(b) H1N1 Infectious classes. $R_{02} > 1$.

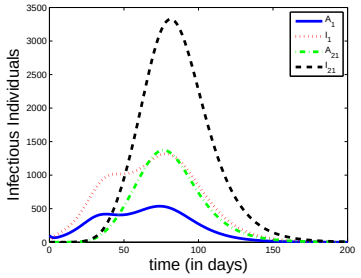

(c) Seasonal Infectious classes. $R_{01} > 1$.

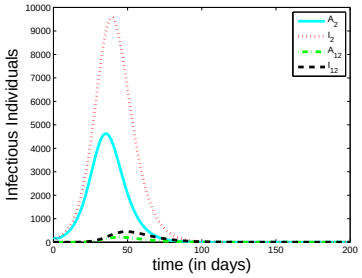

(d) H1N1 Infectious classes. $R_{02} > 1$.

FIGURE 5. Dynamics of the infectious classes in the absence of a vaccination policy where $A_1(0) = 200$ and $A_2(0) = 100$ in Figures (a) and (b), and $A_1(0) = 100$ and $A_2(0) = 200$ in Figures (c) and (d).

Resources are never explicitly limited in our model. However, we want to use a vaccination strategy that conserves vaccines, so we choose the policy: if symptomatic within a recent (pre-determined) window in time, then no vaccine is administered. Specifically, under our vaccination strategy, only those who have never shown influenza symptoms during the ongoing outbreak or who have not received

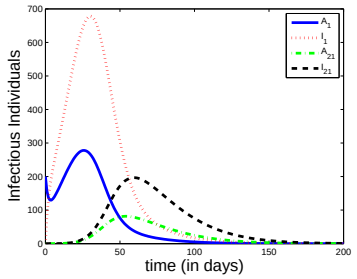

(a) Seasonal Infectious classes. $R_{01v} > 1$.

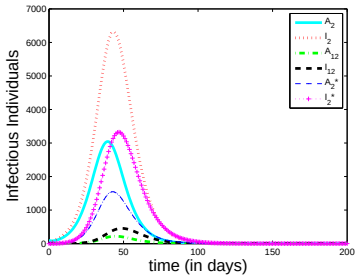

(b) H1N1 Infectious classes. $R_{02v} > 1$.

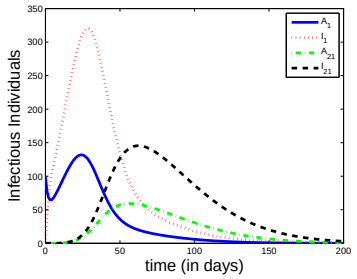

(c) Seasonal Infectious classes. $R_{01v} > 1$.

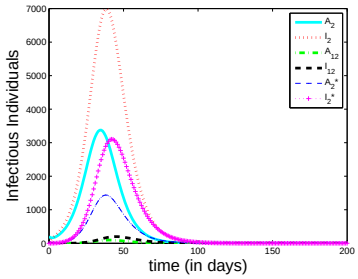

(d) H1N1 Infectious classes. $R_{02v} > 1$.

FIGURE 6. Dynamics of the infectious classes in the presence of the "asymptomatics-only" vaccination policy. In Figures (a) and (b), $A_1(0) = 200$ and $A_2(0) = 100$. In Figures (c) and (d), $A_1(0) = 100$ and $A_2(0) = 200$.

TABLE 3. Results for varying initial conditions (in percentages) with seasonal influenza "asymptomatics-only" vaccination policy

	$A_1(0) = 200$ $A_2(0) = 100$	$A_1(0) = 100$ $A_2(0) = 200$	$A_1(0) = 100$ $A_2(0) = 0$	$A_1(0) = 0$ $A_2(0) = 100$
Population Vaccinated	49	48	95	51
Vaccines Wasted	0.2	0.1	0.1	0
Vaccines Successful	99.8	99.9	99.9	100
Vaccines administered to asymptomatic H1N1 infected individuals	1.9	2.1	0	1.9
Population infected with seasonal	7.7	4.9	4.9	0
Population infected with H1N1	73	73	0	73

a vaccine for the current influenza season will be vaccinated. There will always be wasted vaccines in this strategy since invariably a portion of individuals who are already infected with seasonal influenza but have not yet shown symptoms (A_1) will be vaccinated. To count the total number or fraction of vaccines wasted, we calculate the total number of people who have passed through the vaccinated asymptomatic seasonal compartment (V_{A1}) during the outbreak. Since the vaccination rate (0.01) is low in comparison to the rate of becoming symptomatic (0.5),

TABLE 4. Results (in percentages) for varying initial conditions without vaccination

	$A_1(0) = 200$ $A_2(0) = 100$	$A_1(0) = 100$ $A_2(0) = 200$	$A_1(0) = 100$ $A_2(0) = 0$	$A_1(0) = 0$ $A_2(0) = 100$
Population infected with seasonal	54	57	59	73
Population infected with H1N1	70	71	0	73

a low number of wasted vaccine, less than 1% for each set of initial conditions, is observed (Table 3). Our strategy also allows us to vaccinate those H1N1 asymptomatics as well as those with no previous influenza infections. These vaccinations are successful vaccinations since once a person recovers from H1N1, they would have become susceptible to seasonal influenza were they not to receive the seasonal vaccine. By counting the number of individuals who have traveled through V_{A2} during the outbreak, it was found that this strategy successfully vaccinated a slightly larger percentage (around 2%) of novel A-H1N1 infected individuals (A_2) than the proportion of vaccines wasted (less than 1%) on seasonal influenza asymptomatics (see Figure 7 and Table 3). However, because there is no way to differentiate between seasonal influenza and H1N1 influenza symptoms, this vaccination strategy will also fail to vaccinate those who have not been infected with seasonal influenza but are H1N1-symptomatic (I_2) or have recovered from H1N1 (R_2). This strategy might be useful in societies with limited resources that cannot administer tests for H1N1 to their patients and cannot afford to waste the available vaccines.

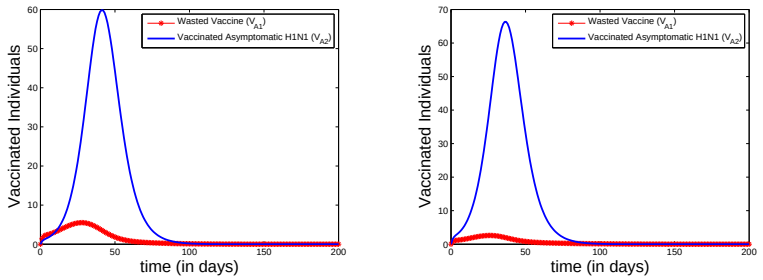

(a) V_{A1} (Wasted Vaccine) and V_{A2} (b) V_{A1} (Wasted Vaccine) and V_{A2}

FIGURE 7. Comparison of vaccines wasted and vaccines administered to H1N1 infected individuals over time. In (a) $A_1(0) = 200$ and $A_2(0) = 100$, in (b) $A_1(0) = 100$ and $A_2(0) = 200$.

The introduction of our seasonal influenza "asymptomatics-only" vaccination program significantly changes the dynamics of the seasonal influenza infections. In the absence of vaccination, as previously explained, more individuals contract secondary (I_{21}) seasonal infections than primary (I_1) seasonal infections. However, when vaccination is introduced, we observed a higher peak in the primary seasonal infections than in the secondary seasonal infections. Since our model assumes no co-infection of influenza virus strains, using the seasonal vaccine has a negative effect

in terms of the H1N1 outbreak. Allowing more individuals to become infected with seasonal influenza, by withholding vaccination, reduces the number of people susceptible to H1N1. Thus, we observe a slight increase in the fraction of the population infected with H1N1 (when vaccination is present) from 70% to 73% for initial conditions $A_1(0) = 200$ and $A_2(0) = 100$, and an increase from 71% to 73% for initial conditions $A_1(0) = 100$ and $A_2(0) = 200$.

3.2. **Optimal control theory applied to two-strain model.** Our goal is to reduce the number of seasonal and H1N1 infections and increase the number of recovered individuals. We used the same technique as with the SAIR model for deriving the optimal control pair (u_1^*, u_2^*). The objective function to be minimized is therefore

$$\mathbb{J}(u_1, u_2) = \int_0^{t_f} [J_1(t)N + J_2(t)N + \frac{B_1}{2}u_1^2(t) + \frac{B_2}{2}u_2^2(t)]dt,$$

where u_1 is controlling β_1 and β_2 and u_2 is controlling γ_2. From Pontryagin's Maximum Principle, we find the optimal controls by minimizing a Hamiltonian, H, where

$$H = J_1(t)N + J_2(t)N + \tfrac{B_1}{2}u_1^2 + \tfrac{B_2}{2}u_2^2 + \sum_{i=1}^{17} \lambda_i g_i.$$

Also, from using Pontryagin's Maximum Principle, we gather that

$$\frac{d\lambda_1}{dt} = -\frac{\partial H}{\partial S}, \lambda_1(t_f) = 0$$
$$\cdots$$
$$\frac{d\lambda_{17}}{dt} = -\frac{\partial H}{\partial P}, \lambda_{17}(t_f) = 0.$$

From this expression, we obtain the adjoint system (See Appendix).
The optimal control pair (u_1^*, u_2^*) is defined by:

$$\begin{aligned} u_1^* &= min(max(LB_1, -\frac{1}{B_1}(\lambda_1(\beta_1 S J_1 + \beta_2 S J_2) + \lambda_2(-\beta_1 S J_1) + \\ &\quad \beta_2 R_1 J_2(\lambda_4 - \lambda_5) + \lambda_7(-\beta_2 S J_2) + \beta_1 R_2 J_1(\lambda_9 - \lambda_{10}) + \\ &\quad \beta_2 V_s J_2(\lambda_{14} - \lambda_{15}))), UB_1) \\ u_2^* &= min(max(LB_2, \frac{\gamma_2}{B_2}(\lambda_6 I_{12} + I_2(\lambda_8 - \lambda_9) + I_2^*(\lambda_{13} - \lambda_{17}))), UB_2); \end{aligned}$$

where LB_i and UB_i are fixed values in $[0, 1]$, $i = 1, 2$.

3.2.1. *Numerical Results.* In this section, we analyzed numerically an optimal control strategy applied to our two-strain influenza model. As in the SAIR Optimal Control Section, we select representative numerical simulations to illustrate the results of applying optimal controls to our two-strain model under three scenarios: one in which social distancing and treatment measures are implemented simultaneously, one in which only social distancing is used, and finally, one in which only treatment is used. We consider each scenario with our "asymptomatics-only" vaccination policy, and without this policy. For the figures and tables presented, we assumed that the number of asymptomatic seasonal infected individuals and the number of asymptomatic H1N1 infected individuals is 100 at time $t = 0$. We again use the parameter values listed in Table 2. Thus, since we have shown that $R_0 = max\{R_{01}, R_{02}\}$, we have that $R_0 = 1.8$.

The first scenario illustrates the effects of increasingly higher costs of social distancing relative to treatment. We select simulations where $B_2 = 10$ is fixed and the cost of implementing social distancing is either two, ten, or one hundred times greater than that of treatment. We ran these simulations for a time span of 100 days and present our results for $\frac{B_1}{B_2} = 2$, $\frac{B_1}{B_2} = 10$, and $\frac{B_1}{B_2} = 100$.

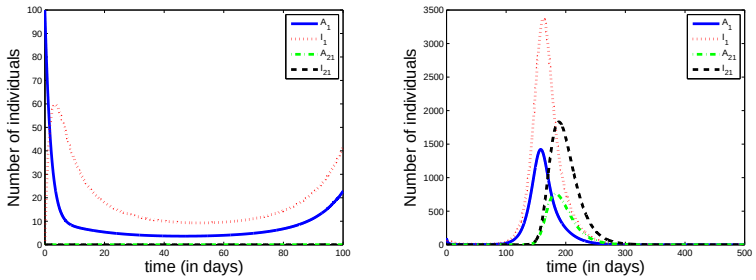

(a) $\frac{B_1}{B_2} = 100$, 100 day window (b) $\frac{B_1}{B_2} = 100$, 500 day window

FIGURE 8. Dynamics of the seasonal influenza classes when $\frac{B_1}{B_2} = 100$, and vaccination is not present.

In general, higher relative social distancing costs (that is, higher $\frac{B_1}{B_2}$ values) resulted in an increase in the total number of influenza cases. In particular, we consistently observed higher numbers of seasonal influenza cases than H1N1 cases. However, when vaccination is eliminated from the model, a greater disparity between the number of seasonal and the number of H1N1 influenza cases appears. When social distancing is assumed to be 100 times more costly than treatment ($\frac{B_1}{B_2} = 100$), and vaccination is not present, seasonal influenza cases begin increasing approximately half-way through the 100 day time period (see Figure 8(a)). Figure 8(b), in which we plot the seasonal infection dynamics for a 500 day window for the same control policy ($(u_1^*, u_2^*) = (0, 0)$ after day 100), demonstrates that this policy only delays the outbreak. This increase means that if the cost of social distancing relative to the cost of treatment is significantly higher, public health programs may need to maintain control measures for a period longer than 100 days to completely stifle the outbreak in the absence of a seasonal influenza vaccination program. In addition to the evident changes in the dynamics of the seasonal influenza classes, as $\frac{B_1}{B_2}$ increases, significant qualitative changes in the corresponding optimal control functions are observed. When the cost of social distancing is twice that of treatment, greater effort should be placed in social distancing rather than treatment, despite its higher cost. However, as we continue to increase this relative cost, we observe that treatment eventually becomes the more dominant control measure - becoming more important as $\frac{B_1}{B_2}$ gets larger. This switch in the roles of social distancing and treatment, which occurred in the cases where $\frac{B_1}{B_2} = 10$ and $\frac{B_1}{B_2} = 100$, indicates that there is a transition point where the cost of social distancing is so great that the optimal control strategy is the one that puts more effort on treatment.

Figure 9(a) illustrates the optimal control strategy without vaccination when $\frac{B_1}{B_2} = 2$. These results showed that in order to reduce the duration and intensity of the outbreak, treatment and social distancing efforts must be kept at a maximum through the peaks of the infectious classes. Following the peak, social distancing

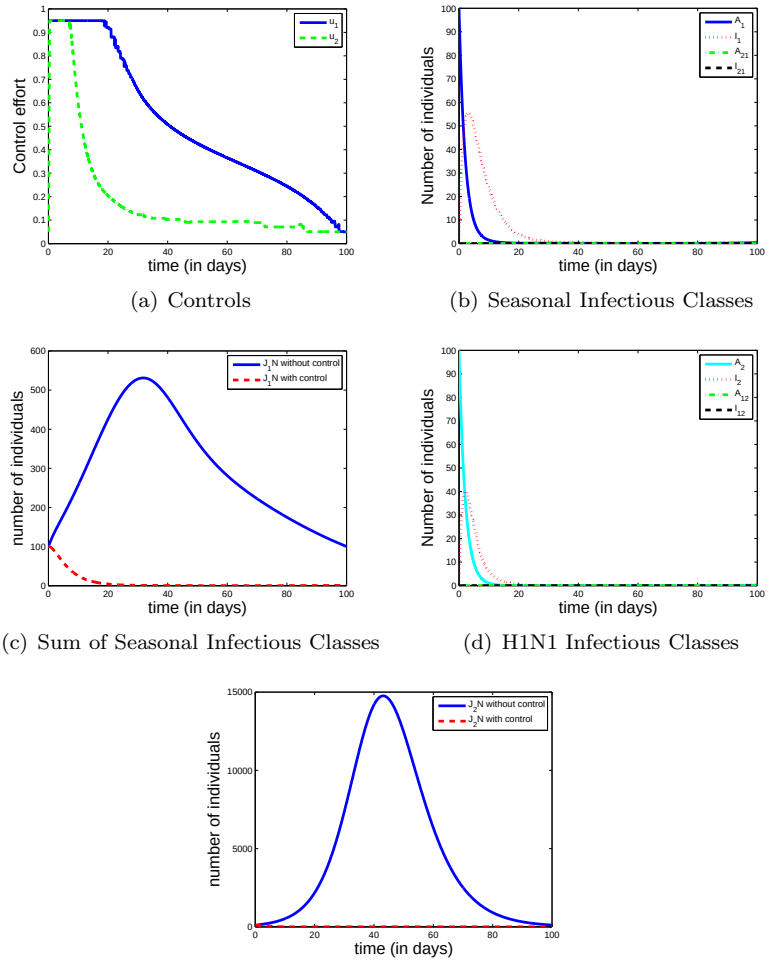

(a) Controls

(b) Seasonal Infectious Classes

(c) Sum of Seasonal Infectious Classes

(d) H1N1 Infectious Classes

(e) Sum of H1N1 Infectious Classes

FIGURE 9. Optimal control results in the absence of a vaccination policy for the case where $\frac{B_1}{B_2} = 2$.

remains at 95% (the prescribed upper bound) for 10 days to suppress the number of influenza infections while the treatment effort diminishes after the outbreak climax. The controls are so effective that they nearly eliminate the occurrence of secondary infections (see Figures 9(b) and 9(d)). In other words, under the optimal control policy, it becomes rare that an individual acquire both a seasonal and a novel H1N1 infection. Since control u_1 hinders the ability of the virus to spread, we can surmise that it is more effective than control u_2, which is supported by our simulations of the optimal control pair. The simulations in Figures 9(c) and 9(e) illustrate the differences in both severity and duration of the seasonal and novel H1N1 epidemics with and without the implementation of controls for the case where $\frac{B_1}{B_2} = 2$. The corresponding graphs of the number of infections over time for $\frac{B_1}{B_2} = 10$ and for $\frac{B_1}{B_2} = 100$ are qualitatively very similar to the case when $\frac{B_1}{B_2} = 2$.

The optimal control strategy in the presence of the "asymptomatics-only" seasonal influenza control policy is one in which control u_2 remains at a maximum effort level for the same period of time as the model without vaccination and control u_1 is maintained at a maximum for a shorter time span. Under the influence of our vaccination strategy, the presence of controls results in a similar impact on the total H1N1 infections as in the absence of vaccination, while seasonal influenza manages to influence a larger proportion of the infected population. However, if the controls were not present, the vaccine still plays an important part in minimizing the seasonal influenza outbreak. We observed that in the presence of vaccination, the optimal control results suggest that more effort should be placed in treatment than when vaccination is absent from the system. This result is consistent with our earlier finding that H1N1 cases increase in the presence of vaccination.

Implementing social distancing exclusively (scenario two) produces similar results to using social distancing in conjunction with treatment, with only slightly higher numbers of influenza cases under the various conditions we explored. In fact, social distancing alone and the simultaneous implementation of the two control measures both resulted in a more than 99% reduction in the number of influenza cases during the control period. In a social-distancing-only control strategy, we also observe qualitative changes in the optimal control function u_2 as the cost of social distancing is increased. As B_1 increases, the duration for which we should implement social distancing at maximum effort at the beginning of the outbreak decreases. For the case where $B_1 = 20$, the optimal control function is at a maximum for just over 20 days. When $B_1 = 100$, our results suggest that maximum effort should be placed for more than 10 days. In the scenario where $B_1 = 1000$, the greatest amount of effort placed in social distancing should be a little below 0.9, at the beginning of the outbreak, and for roughly no more than 5 days.

Employing an influenza control program with only treatment (the third scenario) is significantly less effective than a combination of social distancing and treatment, or even social distancing alone. Regardless of whether or not the model includes vaccination, the optimal treatment-only control strategy actually increases the number of seasonal influenza cases by between 13 and 16 percent. Conversely, novel H1N1 cases decrease by 63 or 73 percent, depending on whether or not our vaccination strategy is executed. With vaccination and treatment, the total number of influenza cases is reduced by 59%. Without vaccination, treatment-only control results in a 37% reduction in the number of influenza cases. Since vaccination alone results in a reduction of cases (compared with no vaccination) by approximately 35% over the 100 day period, using treatment as a control measure may still be worthwhile if social distancing is not feasible. According to our model, if vaccines are not available, treatment could be used as a substitute for vaccination, producing similar results.

While treatment reduces morbidity under any of the scenarios we have considered, concerns regarding the potential for the novel H1N1 virus to develop drug-resistance may deter some policy makers from choosing a control strategy which relies heavily on the use of antivirals.

4. **Conclusions and future work.**

Fortunately, the novel A-H1N1 virus that emerged in Mexico in the spring of 2009 never reached its full pandemic potential. However, managing this epidemic still induced large economic costs, particularly for poor and developing nations such as Mexico, and brought to the forefront the need to develop epidemic control strategies that not only minimize the morbidity

and mortality of an outbreak, but also the need to develop strategies that are economically feasible for any country. Addressing this problem by applying optimal control theory to the SAIR model for novel H1N1 allowed us to determine optimal strategies for minimizing the H1N1 outbreak in a cost-effective manner. Using a combination of social distancing and treatment, the optimal strategy reduced the number of H1N1 infections by more than 99% during the 100-day control period; social distancing alone produced similar results. However, the optimal treatment-only strategy only reduced morbidity by 63% when the cost was low. This percentage decreases as the cost of treatment increases.

While the SAIR model provided some insights into what an optimal policy for the novel A-H1N1 epidemic might be, we recognized that the presence of the seasonal influenza epidemic, which also poses a significant health risk each year, might further complicate the problems associated with H1N1. The numerical results and simulations for the concurrent influenza epidemic model showed that administering the seasonal influenza vaccine according to our "asymptomatics-only" vaccination policy reduced the overall number of infectious individuals in an outbreak and kept the number of wasted vaccines low. However, this strategy increased the number of H1N1 infections. This increase is a byproduct of our model assumption that an individual cannot be co-infected with a seasonal and a novel H1N1 influenza virus. We also observed that when the initial population of those infected with seasonal influenza is larger than that of H1N1, more vaccines are wasted.

Using optimal control theory, we determined that implementing treatment and social distancing control measures optimally has a substantial effect on controlling the number of infections during an outbreak. When social distancing begins, the number of infectious individuals rapidly declines. The controls are so effective in suppressing the spread of infection that they nearly eliminated secondary influenza infection cases from arising. That is, individuals who acquire both seasonal and novel H1N1 infections are rare under the optimal control policy. The optimal implementation of both social distancing alone and social distancing in conjunction with treatment resulted in a more than 99% reduction in the total number of influenza cases. The optimal treatment-only strategy reduced cases by 59% in the presence of vaccination, and by 37% in the absence of vaccination. Although social distancing is more effective than treatment in controlling the disease, the effort placed in treatment became more important in the presence of vaccination as well as when the cost of social distancing increased relative to the cost of treatment.

When vaccination is eliminated from the model and the cost of social distancing relative to treatment is high ($\frac{B_1}{B_2}$=100), we observed that implementing control measures for a 100-day time period was not long enough to suppress the influenza outbreak. In fact, since the optimal control policy over this time period does not, in any of the scenarios we examined, reduce the number of infectious cases to zero by the 100th day, we expect to see an outbreak occur once control measures are lifted. With control measures removed, the basic reproductive number R_0 returns to its original value of 1.8. An R_0 value greater than one, along with a positive number of infections will lead to an outbreak. However, in the case where both social distancing and treatment controls are used with $\frac{B_1}{B_2} = 2$, and the "asymptomatics-only" vaccination policy is in place, the number of individuals in each infected class is between zero and one. For practical purposes we can treat "less than one" of an individual as zero individuals. Thus, in this scenario, we may assume that the corresponding 100-day optimal control policy successfully eliminated the

threat of an influenza outbreak occurring after the control measures are lifted. In the remaining scenarios, although we cannot entirely prevent an outbreak from occurring once control measures are lifted after only 100 days, extending the control period would either mitigate the severity of the delayed outbreak, or if the control period is extended sufficiently, bring the number of cases in each infectious class below one by the end of the control period.

It is likely that even if the optimal control policy is known, that policy may not be implemented precisely, or resources to implement the optimal policy may be limited. While Lee et al. consider the problem of limited resources in an optimal control problem using different, and more rigorous, techniques [24], we considered what impact a 10, 20, 40, or 50 percent reduction in the optimal control effort might have on the dynamics of a concurrent influenza outbreak. We present in Figure 10 the results for the scenario where social distancing and treatment measures are implemented simultaneously. Initially, the number of infected individuals decreases as it does when the optimal controls are implemented perfectly. However, the number of cases begins to rise again, indicating that using a strategy less than the optimal strategy has the effect of simply delaying the outbreak if we restrict our policy to a 100-day window in time. During the 2009-2010 novel H1N1 epidemic, the late arrival of novel H1N1 vaccines was of great concern. Thus, although it may be unrealistic to completely prevent an outbreak from occurring using control measures such as social distancing and treatment over a 100-day period, simply delaying the outbreak until vaccines arrive might be helpful in mitigating the severity of a pandemic.

Acknowledgments. We would like to thank Gerardo Chowell for his helpful comments, Eunok Jung, Jose Vega-Guzman, Maytee Cruz-Aponte, Emmanuel Rosales, Edme Soho and all other MTBI 2009 faculty for the guidance they provided us in our research. This project has been partially supported by grants from the National Science Foundation (NSF - Grant DMPS-0838704), the National Security Agency (NSA - Grant H98230-09-1-0104), the Alfred P. Sloan Foundation and the Office of the Provost of Arizona State University.

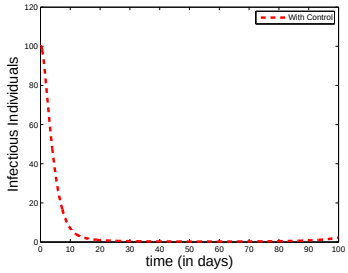

(a) Effect of perfectly implemented optimal control policy (u_1^*, u_2^*) on epidemic

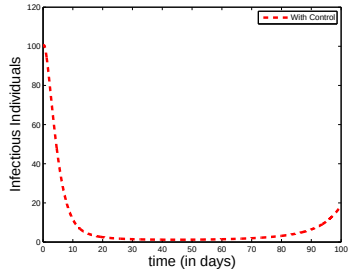

(b) Effect of 10% reduction in (u_1^*, u_2^*) on epidemic

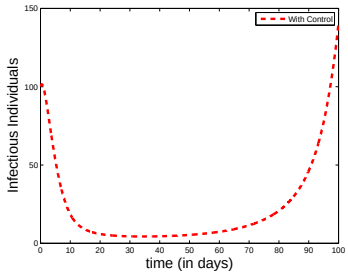

(c) Effect of 20% reduction in (u_1^*, u_2^*) on epidemic

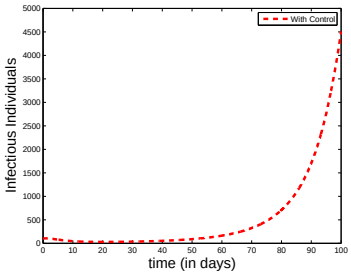

(d) Effect of 40% reduction in (u_1^*, u_2^*) on epidemic

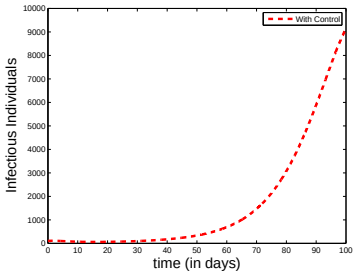

(e) Effect of 50% reduction in (u_1^*, u_2^*) on epidemic

FIGURE 10. Effect of 0, 10, 20, 40, or 50 percent reduction in (u_1^*, u_2^*) on epidemic.

REFERENCES

[1] L. Altman, "Many Swine Flu Cases Have no Fever," New York Times, 2009.

[2] R. M. Anderson and R. M. May, "Infectious Diseases of Humans," Oxford University Press, Oxford, 1991.

[3] I. G. Barr, J. McCauley, N. Cox, R. Daniels, O. G. Engelhardt, K. Fukuda, G. Grohmann, A. Hay, A. Kelso, A. Klimov, T. Odagiri, D. Smith, C. Russell, M. Tashiro, R. Webby, J. Wood, Z. Ye and W. Zhang, *Epidemiological, antigenic and genetic characteristics of seasonal influenzaA(H1N1), A(H3N2) and B influenza viruses: Basis for the WHO recommendation on the composition of influenza vaccines for use in the 20092010 Northern Hemisphere season*, Vaccine, **28** (2010), 1156–1167.

[4] H. Behnke, *Optimal control of deterministic epidemics*, Optimal Control Application Methods, **21** (2000), 269–285.

[5] W. I. B. Beveridge, "Influenza: The Last Great Plague. An Unfinished Story of Discovery," Prodist, 1977.

[6] F. Brauer, Z. Feng and C. Castillo-Chavez, *Discrete epidemic models*, Mathematical Biosciences and Engineering, **7** (2010), 1–15.

[7] C. Castillo-Chavez, H. Hethcote, V. Andreason, S. A. Levin and W. M. Liu, *Cross-immunity in the dynamics of homogeneous and heterogeneous populations*, Mathematical Ecology, (1988), 303–316.

[8] Centers for Disease Control and Prevention (CDC), *Key facts about seasonal influenza*, http://www.cdc.gov/flu/keyfacts.htm.

[9] Centers for Disease Control and Prevention (CDC), *Monitoring influenza activity, including 2009 H1N1*, (2009), Monitoring Influenza Activity, Including 2009 h1n1.

[10] Centers for Disease Control and Prevention (CDC), *Serum cross-reactive antibody response to a novel influenza A(H1N1) virus after vaccination with seasonal influenza vaccine*, MMWR Morb Mortal Wkly Rep, **58** (2009), 521–524.

[11] G. Chowell, M. A. Miller and C. Viboud, *Seasonal influenza in the United States, France, and Australia: Transmission an prospects for control*, Epidem. Infect., **136** (2008), 852–864.

[12] G. Chowell, S. M. Bertozzi, M. A. Colchero, H. Lopez-Gatell, C. Alpuche-Aranda, M. Hernandez and M. A. Miller, *Severe respiratory disease concurrent with the circulation of H1N1 influenza*, The New England Journal of Medicine, **361** (2009), 674–679.

[13] Brian Coburn, "Multi-species Influenza Models with Recombination," Ph.D thesis, University of Miami in Coral Gables,FL, 2009.

[14] R. Couch and J. Kasel, *Immunity to influenza in man*, Annual Reviews in Microbiology, **37** (2002), 529–549.

[15] O. Diekmann and J. A. P. Heesterbeek, "Mathematical Epidemiology of Infectious Diseases. Model Building, Analysis and Interpretation," John Wiley & Sons, Ltd., Chichester, 2000.

[16] D. J. D. Earn, J. Dushoff and S. A. Levin, *Ecology and evolution of the flu*, Trends Ecol. Evol., **17** (2002), 334–340.

[17] S. Echevarra-Zuno, J. M. Meja-Arangur, A. V. Mar-Obeso, C. Grajales-Muiz, E. Robles-Prez, M. Gonzlez-Len, M. C. Ortega-Alvarez, C. Gonzalez-Bonilla, R. A. Rascn-Pacheco and V. H. Borja-Aburto, *Infection and death from influenza A H1N1 virus in Mexico: A retrospective analysis*, Lancet, **374** (2009), 2072–2079.

[18] A. Esteves-Jaramillo, S. B. Omer and E. Gonzalez-Diaz, *Acceptance of a vaccine against novel influenza A (H1N1) virus among health care workers in two major cities in Mexico*, Archives of Medical Research, **40** (2009), 705–711.

[19] W. H. Fleming and R. W. Rishel, "Deterministic and Stochasitic Optimal Control," Springer-Verlag, New York, 1994.

[20] FLU. GOV, *2009 H1N1 vaccine doses allocated, ordered, and shipped by project area*, (2010), http://www.flu.gov/individualfamily/vaccination/supply.html.

[21] M. A. Herrera-Valdez, M. Cruz-Aponte and C. Castillo-Chavez, *Multiple waves for the same pandemic: Local transportation and social distancing explain the dynamics of the A/H1N1 epidemic during 2009 in Mexico*, (2010).

[22] E. Jung, S. Lenhart and Z. Feng, *Optimal control of treatments in a two-strain tuberculosis model*, Discrete and Continuous Dynamical Systems-Series B, **2** (2002), 473–482.

[23] P. Y. Lee, D. B. Matchar, D. A. Clements, J. Huber, J. D. Hamilton and E. D. Peterson, *Economic analysis of influenza vaccination and antiviral treatment for healthy working adults*, Ann. Intern. Med., **137** (2002), 225–231.

[24] S. Lee, G. Chowell and C. Castillo-Chavez, *Optimal control of influenza pandemics: the role of antiviral treatment and isolation*, Journal of Theoretical Biology, **265** (2010), 136–150.

[25] S. Lenhart and J. T. Workman, "Optimal Control Applied to Biological Models," Chapman & Hall/CRC Mathematical and Computational Biology Series, 2007.

[26] E. Malkin, *Flu? What flu?*, The New York Times, http://www.nytimes.com/2009/05/09/business/global/09peso.html.

[27] H. Nishiura, C. Castillo-Chavez, M. Safan and G. Chowell, *Transmission potential of the new Influenza A(H1N1) virus and its age-specificity in Japan*, Eurosurveillance, **14** (2009), 1–4.

[28] M. Nuno, G. Chowell and A. B. Gumel, *Assessing the role of basic control measures, antivirals and vaccine in curtailing pandemic influenza: Scenarios for the US, UK and the Netherlands*, Journal of The Royal Society Interface, **4** (2007), 505–521.

[29] J. Plotkin, J. Dushoff and S. Levin, *Hemagglutinin sequence clusters and the antigenic evolution of influenza A virus*, Proceedings of the National Academy of Sciences, **99** (2002), 6263–6268.

[30] L. S. Pontryagin, R. V. Boltyanski, R. V. Gamkrelidge and E. F. Mischenko, "The Mathematical Theory of Optimal Processes," John Wiley and Sons, N.Y., 1962.

[31] Prevent Influenza Now! Sponsored by the National Influenza Vaccine Summit, *Influenza vaccine availability tracking system (IVATS)*, http://www.preventinfluenza.org/ivats/.

[32] C. E. Shoichet, *Mexico still waiting for most swine flu vaccines*, (2010), http://www.boston.com/business/articles/2010/01/13/mexico_still_waiting_for_most_swine_flu_vaccines/.

[33] E. Spackman, D. Stallknecht, R. Slemons, K. Winker, D. L. Suarez, M. Scott and D. E. Swayne, *Phylogenetic analyses of type A influenza genes in natural reservoir species in North America reveals genetic variation*, Virus research, **114** (2005), 89–100.

[34] R. Stengel, *Optimal control and estimation*, http://www.princeton.edu/ stengel/MAE546.html.

[35] T. Suess, U. Buchholz, S. Dupke, R. Grunow, M. an der Heiden, A. Heider, B. Biere, B. Schweiger, W. Haas and G. Krause, *Shedding and transmission of novel influenza virus A/H1N1 infection in householdsGermany, 2009*, American Journal of Epidemiology, **171** (2010), 1157–1164.

[36] J. K. Taubenberger, D. M. Morens, *1918 influenza: the mother of all pandemics*, Emerging Infectious Diseases, (2009), http://www.cdc.gov/ncidod/EID/vol12no01/05-0979.htm.

[37] P. van den Driessche and J. Watmough, *Reproduction numbers and sub-threshold endemic equilibria for compartmental models of disease transmission*, Mathematical Biosciences, **180** (2002), 29–48.

[38] World Health Organization, *Recommended composition of influenza of influenza virus vaccines for use in the 2001-2002 season*, Wkly. Epidemiol. Rec., **76** (2001), 58–61.

Appendix.

Proof of Theorem 2.1. The existence of an optimal control pair follows from Corollary 4.1 of [19] and the following two facts: the integrand of J is convex with respect to (u_1, u_2) and the state system is *Lipshitz* with respect to the state variables. The following relationships follow directly from the application of Pontryagin's Maximum Principle [30]:

$$\frac{d\lambda_1(t)}{dt} = -\frac{\partial H}{\partial S}, \ \frac{d\lambda_2(t)}{dt} = -\frac{\partial H}{\partial D}, \ \frac{d\lambda_3(t)}{dt} = -\frac{\partial H}{\partial R}, \ \frac{d\lambda_4(t)}{dt} = -\frac{\partial H}{\partial R},$$

with $\lambda_i(t_f) = 0$ for $i = 1, 2, 3$, and 4 evaluated at the optimal control pair and corresponding states. These evaluations naturally lead to the Adjoint System (11). The Hamiltonian H must be minimized with respect to the controls at the optimal control pair and so we differentiate H with respect to u_1 and u_2 on the set Ω. These computations lead to the following optimality conditions:

$$\frac{\partial H}{\partial u_1} = B_1 u_1 + (\lambda_1 - \lambda_2)\beta S \left(\frac{A+I}{N}\right) = 0 \text{ at } u_1 = u_1^*$$

and

$$\frac{\partial H}{\partial u_2} = B_2 u_2 + (-\lambda_3 + \lambda_4)\gamma_T I = 0 \text{ at } u_1 = u_1^*.$$

Solving for u_1^* and u_2^* gives

$$\begin{aligned} u_1^* &= \frac{1}{B_1}\left[\beta S\left(\frac{A+I}{N}\right)(\lambda_2 - \lambda_1)\right], \\ u_2^* &= \frac{1}{B_2}\left[\gamma_T I(\lambda_3 - \lambda_4)\right], \end{aligned}$$

Use of the bounds on $LB_i \leq u_i \leq UB_i$ for $i = 1, 2$ lead to the expressions in (13). □

Adjoint system for two-strain model with controls.

$$\begin{aligned}
\frac{d\lambda_1}{dt} &= \lambda_1(\beta_1(1-u_1^*)J_1 + \beta_2(1-u_1^*)J_2 + \nu) - \lambda_2(\beta_1(1-u_1^*)J_1) \\
&\quad -\lambda_7(\beta_2(1-u_1^*)J_2) - \lambda_{14}(\nu) \\
\frac{d\lambda_2}{dt} &= -1 + \lambda_1(\beta_1(1-u_1^*)\frac{S}{N}) - \lambda_2(\beta_1(1-u_1^*)\frac{S}{N} - (\alpha_1+\nu)) - \lambda_3(\alpha_1) \\
&\quad +\lambda_9(\beta_1(1-u_1^*)\frac{R_2}{N}) - \lambda_{10}(\beta_1(1-u_1^*)\frac{R_2}{N}) - \lambda_{16}(\nu) \\
\frac{d\lambda_3}{dt} &= -1 + \lambda_1(\beta_1(1-u_1^*)\frac{S}{N}) - \lambda_2(\beta_1(1-u_1^*)\frac{S}{N}) + \lambda_3(\gamma_1+\mu_1) - \lambda_4(\gamma_1) \\
&\quad +\lambda_9(\beta_1(1-u_1^*)\frac{R_2}{N}) - \lambda_{10}(\beta_1(1-u_1^*)\frac{R_2}{N}) \\
\frac{d\lambda_4}{dt} &= \lambda_4(\beta_2(1-u_1^*)J_2) - \lambda_5(\beta_2(1-u_1^*)J_2) \\
\frac{d\lambda_5}{dt} &= -1 + \lambda_1(\beta_2(1-u_1^*)\frac{S}{N}) + \lambda_4(\beta_2(1-u_1^*)\frac{R_1}{N}) \\
&\quad -\lambda_5(\beta_2(1-u_1^*)\frac{R_1}{N} - \alpha_2) - \lambda_6(\alpha_2) - \lambda_7(\beta_2(1-u_1^*)\frac{S}{N}) \\
&\quad +\lambda_{14}(\beta_2(1-u_1^*)\frac{V_S}{N}) - \lambda_{15}(\beta_2(1-u_1^*)\frac{V_S}{N}) \\
\frac{d\lambda_6}{dt} &= -1 + \lambda_1(\beta_2(1-u_1^*)\frac{S}{N}) + \lambda_4(\beta_2(1-u_1^*)\frac{R_1}{N}) - \lambda_5(\beta_2(1-u_1^*)\frac{R_1}{N}) \\
&\quad +\lambda_6(\gamma_2(1+u_2^*) + \mu_2) - \lambda_7(\beta_2(1-u_1^*)\frac{S}{N}) + \lambda_{14}(\beta_2(1-u_1^*)\frac{V_S}{N}) \\
&\quad -\lambda_{15}(\beta_2(1-u_1^*)\frac{V_S}{N}) - \lambda_{17}(\gamma_2(1+u_2^*)) \\
\frac{d\lambda_7}{dt} &= -1 + \lambda_1(\beta_2(1-u_1^*)\frac{S}{N}) + \lambda_4(\beta_2(1-u_1^*)\frac{R_1}{N}) - \lambda_5(\beta_2(1-u_1^*)\frac{R_1}{N}) \\
&\quad -\lambda_7(\beta_2(1-u_1^*)\frac{S}{N} + (\alpha_2+\nu)) - \lambda_8(\alpha_2) - \lambda_{12}(\nu) \\
&\quad +\lambda_{14}(\beta_2(1-u_1^*)\frac{V_S}{N}) - \lambda_{15}(\beta_2(1-u_1^*)\frac{V_S}{N})
\end{aligned}$$

$$
\begin{aligned}
\frac{d\lambda_8}{dt} &= -1+\lambda_1(\beta_2(1-u_1^*)\frac{S}{N})+\lambda_4(\beta_2(1-u_1^*)\frac{R_1}{N})-\lambda_5(\beta_2(1-u_1^*)\frac{R_1}{N}) \\
&\quad -\lambda_7(\beta_2(1-u_1^*)\frac{S}{N})+\lambda_8(\gamma_2(1+u_2^*)+\mu_2)-\lambda_9(\gamma_2(1+u_2^*)) \\
&\quad +\lambda_{14}(\beta_2(1-u_1^*)\frac{V_S}{N})-\lambda_{15}(\beta_2(1-u_1^*)\frac{V_S}{N}) \\
\frac{d\lambda_9}{dt} &= \lambda_9(\beta_1(1-u_1^*)J_1)-\lambda_{10}(\beta_1(1-u_1^*)J_1) \\
\frac{d\lambda_{10}}{dt} &= -1+\lambda_1(\beta_1(1-u_1^*)\frac{S}{N})-\lambda_2(\beta_1(1-u_1^*)\frac{S}{N})+\lambda_9(\beta_1(1-u_1^*)\frac{R_2}{N}) \\
&\quad -\lambda_{10}(\beta_1(1-u_1^*)\frac{R_2}{N}-\alpha_1)-\lambda_{11}(\alpha_1) \\
\frac{d\lambda_{11}}{dt} &= -1+\lambda_1(\beta_1(1-u_1^*)\frac{S}{N})-\lambda_2(\beta_1(1-u_1^*)\frac{S}{N})+\lambda_9(\beta_1(1-u_1^*)\frac{R_2}{N}) \\
&\quad -\lambda_{10}(\beta_1(1-u_1^*)\frac{R_2}{N})+\lambda_{11}(\gamma_1+\mu_1)-\lambda_{17}(\gamma_1) \\
\frac{d\lambda_{12}}{dt} &= -1+\lambda_1(\beta_2(1-u_1^*)\frac{S}{N})+\lambda_4(\beta_2(1-u_1^*)\frac{R_1}{N})-\lambda_5(\beta_2(1-u_1^*)\frac{R_1}{N}) \\
&\quad -\lambda_7(\beta_2(1-u_1^*)\frac{S}{N})+\lambda_{12}(\alpha_2^*)-\lambda_{13}(\alpha_2^*)+\lambda_{14}(\beta_2(1-u_1^*)\frac{V_S}{N}) \\
&\quad -\lambda_{15}(\beta_2(1-u_1^*)\frac{V_S}{N}) \\
\frac{d\lambda_{13}}{dt} &= -1+\lambda_1(\beta_2(1-u_1^*)\frac{S}{N})+\lambda_4(\beta_2(1-u_1^*)\frac{R_1}{N})-\lambda_5(\beta_2(1-u_1^*)\frac{R_1}{N}) \\
&\quad -\lambda_7(\beta_2(1-u_1^*)\frac{S}{N})+\lambda_{13}(\gamma_2(1+u_2^*)+\mu_2)+\lambda_{14}(\beta_2(1-u_1^*)\frac{V_S}{N}) \\
&\quad -\lambda_{15}(\beta_2(1-u_1^*)\frac{V_S}{N})-\lambda_{17}(\gamma_2(1+u_2^*)) \\
\frac{d\lambda_{14}}{dt} &= -\lambda_{15}(\beta_2(1-u_1^*)J_2)+\lambda_{14}(\beta_2(1-u_1^*)J_2) \\
\frac{d\lambda_{15}}{dt} &= -1+\lambda_1(\beta_2(1-u_1^*)\frac{S}{N})+\lambda_4(\beta_2(1-u_1^*)\frac{R_1}{N})-\lambda_5(\beta_2(1-u_1^*)\frac{R_1}{N}) \\
&\quad -\lambda_7(\beta_2(1-u_1^*)\frac{S}{N})-\lambda_{13}(\alpha_2)+\lambda_{14}(\beta_2(1-u_1^*)\frac{V_S}{N}) \\
&\quad -\lambda_{15}(\beta_2(1-u_1^*)\frac{V_S}{N}-\alpha_2) \\
\frac{d\lambda_{16}}{dt} &= -1+\lambda_1(\beta_1(1-u_1^*)\frac{S}{N})-\lambda_2(\beta_1(1-u_1^*)\frac{S}{N})-\lambda_3(\alpha_1^*) \\
&\quad +\lambda_9(\beta_1(1-u_1^*)\frac{R_2}{N})-\lambda_{10}(\beta_1(1-u_1^*)\frac{R_2}{N})+\lambda_{16}(\alpha_1^*) \\
\frac{d\lambda_{17}}{dt} &= 0
\end{aligned}
$$

Received June 30, 2010; Accepted September 11, 2010.

E-mail address: oprosper@ufl.edu;saucedo.omar@yahoo.com
E-mail address: doria_thompson@yahoo.com;griselle@mathpost.asu.edu
E-mail address: Xiaohong.Wang@asu.edu;ccchavez@asu.edu